



1st CIRP Conference on Surface Integrity (CSI)

## Surface Integrity in Dry and Cryogenic Machining of *AZ31B Mg* Alloy with Varying Cutting Edge Radius Tools

Z. Pu<sup>a\*</sup>, J.C. Outeiro<sup>b</sup>, A.C. Batista<sup>c</sup>, O.W. Dillon, Jr.<sup>a</sup>, D.A. Puleo<sup>d</sup>, I.S. Jawahir<sup>a</sup>

<sup>a</sup>*Department of Mechanical Engineering and Institute for Sustainable Manufacturing,  
University of Kentucky, Lexington, KY 40506, USA*

<sup>b</sup>*Faculty of Engineering, Catholic University of Portugal, 2635-631 Rio de Mouro, Sintra, Portugal  
and CEMDRX, University of Coimbra, Rua larga, P-3004 516 Coimbra, Portugal*

<sup>c</sup>*Department of Physics, University of Coimbra, P-3004-516 Coimbra, Portugal*

<sup>d</sup>*Center for Biomedical Engineering, Wenner-Gren Lab, University of Kentucky, Lexington, KY 40506, USA*

---

### Abstract

Surface integrity of machined products has a critical impact on their functional performance. Magnesium alloys are lightweight materials for transportation industry and are also emerging as a potential material for temporary biomedical implants. However, their unsatisfactory corrosion resistance limits their application to a great extent. Surface integrity factors, such as grain size, crystallographic orientation and residual stresses, were reported to have significant influence on corrosion resistance of *AZ31 Mg* alloys. In this study, *AZ31B Mg* discs were orthogonally turned using cutting tools with two edge radii under both dry and cryogenic conditions. The influence of cutting edge radius and cooling method on surface integrity was investigated. Cryogenic machining using a large edge radius tool led to a thicker grain refinement layer, larger compressive residual stresses and stronger intensity of basal texture, which may remarkably enhance the corrosion performance of magnesium alloys.

© 2010 Published by Elsevier Ltd. Selection and/or peer-review under responsibility of [name organizer]

*keywords:* Cryogenic Cooling, Surface Integrity, Magnesium, Crystallographic Orientation.

---

### 1. Introduction

Surface integrity of the machined products has a critical impact on their functional performance [1, 2]. Refinement of grain size near the surface to the nano level was proved to an effective way to enhance the functional performance of various metallic materials, such as the corrosion resistance of stainless steel [3] and fatigue life of a nickel-based hastelloy [4]. Machining, which is a severe plastic deformation (SPD) process involving large strains (typically 2–10) and high strain rates (up to  $10^6 \text{ s}^{-1}$ ), was found recently to be an effective method to introduce grain refinement in a surface layer [5, 6] and has many unique

---

\* Corresponding author. Tel: +001-859-323-3283

E-mail address: [z.pu@uky.edu](mailto:z.pu@uky.edu)

advantages over laboratory-based SPD processes, such as shorter process time, better controllability, cost effective and better surface finish. However, due to the large amount of heat generated during machining, the thickness of the grain refinement surface layer is often very small, which may limit the possible benefits that could be gained from the refined grains.

Magnesium alloys are promising lightweight structural materials for both automotive and aerospace applications. Recently, new application of magnesium alloys as a novel biodegradable material for temporary internal fixation implants is also emerging [7]. However, one major limitation preventing the wide application is their unsatisfactory corrosion performance. Grain refinement was proved to be an effective way to improve the corrosion resistance of magnesium alloys [8]. The high residual compressive stresses generated in the subsurface via a deep rolling process was also claimed to reduce the corrosion rate of a biphasic *MgCa3.0* alloy by a factor of approximately 100 [9]. In addition, recent studies show that crystallographic orientations have remarkable influences on corrosion resistance. It was proved both experimentally and theoretically that the basal plane of *AZ31 Mg* alloy was more corrosion resistant than the other planes due to its higher atomic coordination and thus lower surface energy [10]. Both grain refinement and strong basal texture were claimed to be the causes for improved corrosion resistance after cryogenic burnishing [11].

In this study, the effects of cutting edge radius and cooling methods (dry and cryogenic) on surface integrity in machining of *AZ31B Mg* alloy were investigated. Although the influence of edge radius on residual stresses was often reported [12, 13], this study is among the first to report its influence on crystallographic orientations of machined surfaces. The results show that cryogenic machining with large edge radius led to the most desirable surface integrity in terms of grain size, crystallographic orientation and residual stresses, which should enhance the corrosion resistance of *AZ31 Mg* alloy significantly.

## 2. Experimental Procedures

### 2.1. Machining experiments

The material studied was the commercial *AZ31B-O Mg* alloy. It was obtained in the form of a 3.22 mm thick sheet. Disc specimens (3.22 mm in thickness and 130 mm in diameter) were cut from sheet by vertical milling and subsequently subjected to orthogonal machining. A Mazak Quick Turn-10 Turning Center equipped with an Air Products ICEFLY<sup>®</sup> liquid nitrogen delivery system is used for the machining experiments. The cutting tool used was uncoated carbide. The experimental matrix was shown in Table 1. The edge radius of the cutting tools ( $r_n$ ) was ground to two different values, 30  $\mu\text{m}$  and 70  $\mu\text{m}$ . For cryogenic machining, liquid nitrogen was sprayed to the machined surface at a flow rate of 0.6 kg/min via a nozzle from the clearance side of the cutting tool as shown in Fig.1. The cutting speed used was 100 m/min and the feed rate was 0.1 mm/rev. The rake angle and the clearance angle were both  $-7^\circ$ .

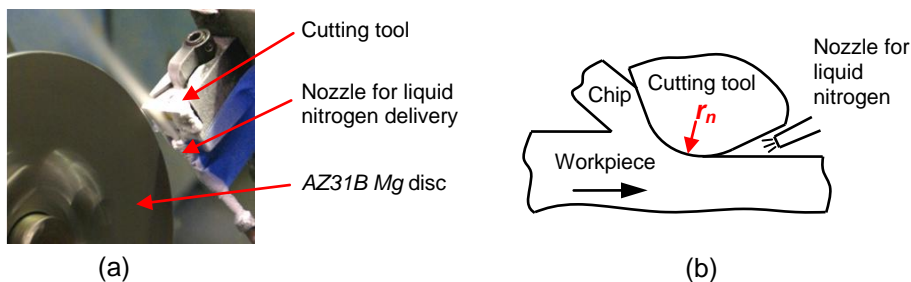


Fig. 1. Experimental setup of cryogenic machining: (a) photo (tool approaching workpiece) and (b) schematic diagram.

Table 1. Matrix for the machining experiments

| Test No.                              | 1   | 2   | 3         | 4         |
|---------------------------------------|-----|-----|-----------|-----------|
| Cooling Method                        | Dry | Dry | Cryogenic | Cryogenic |
| Cutting Edge Radius [ $\mu\text{m}$ ] | 30  | 70  | 30        | 70        |

## 2.2. Characterization of surface integrity

After machining, metallurgical samples were cut from the machined discs. After cold mounting, grinding and polishing, acetic picric solution was used as the etchant to reveal the grain structure. Optical microscopy was used to observe the cross-sectional microstructure of the *AZ31B Mg* discs near the machined surface. The crystallographic orientations on the machined surfaces were analyzed by using a Bruker D8 Discover X-ray diffractometer. The residual stresses in machined *AZ31B Mg* samples were analyzed by X-ray diffraction technique using the  $\sin^2\psi$  method [14]. The equipment used was a PROTO iXRD diffractometer available at the X-ray Diffraction Center for Materials Research (CEMDRX), University of Coimbra, Portugal. The parameters used in the X-ray analysis are shown in Table 2. To determine the in-depth residual stress profiles, successive layers of material were removed by electropolishing to avoid the modification of machining-induced stresses. Further corrections to the residual stress data were made due to the volume of material removed. It is noted that the penetration depth of the X-ray beam in the Mg alloy is about 25  $\mu\text{m}$  for the diffraction parameters used in this study. Therefore, the measured residual stress data started at 25  $\mu\text{m}$  below the machined surface.

Table 2. X-ray diffraction parameters for residual stress measurement of *AZ31B Mg* alloy

| Radiation                      | Bragg angle $2\theta$ [ $^\circ$ ] | X-ray elastic modulus [ $\text{MPa}^{-1}$ ]                            | Number of $\psi$ angles |
|--------------------------------|------------------------------------|--|-------------------------|
| <i>Mn-K<math>\alpha</math></i> | 151.06<br>(hkl) = (203)            | $\frac{1}{2}S_2 = 29.32 \times 10^{-6}$ , $S_1 = -6.59 \times 10^{-6}$ | 30                      |

## 3. Results and Discussions

### 3.1. Microstructural analysis

The microstructure before machining is shown in Fig. 2a. The grain boundaries were clearly visible near the machined surface. Cryogenic machining using the cutting tool with 30  $\mu\text{m}$  edge radius resulted in a surface layer about 8  $\mu\text{m}$  thick in which grain boundaries were no longer visible at this magnification as shown in Fig. 2b. With 70  $\mu\text{m}$  cutting edge radius tool, the thickness increased to 15  $\mu\text{m}$  [15]. Under dry conditions, there were no such layers. The microstructures of other machining conditions was reported in a previous study [15]. Fig. 2c shows the microstructure of the chips from cryogenic machining with 30  $\mu\text{m}$  cutting edge radius tool. While the grain boundaries were clear in the interior of the serrated chips, the grain boundaries disappeared near the tool-chip interface and a “white layer” about 22  $\mu\text{m}$  thick similar to that on the machined surface was formed. This agrees with a recent finding where it was proved experimentally that the tool-chip interface and the machined surface underwent similar deformation in terms of strains and strain rates [5]. Nanocrystallized grains were reported on the “white layer” of *AISI 52100* steel [16]. It was also reported that the “white layer” of *AZ31B Mg* alloy after cryogenic machining also consisted of nanocrystallized grains about 45 nm [17].

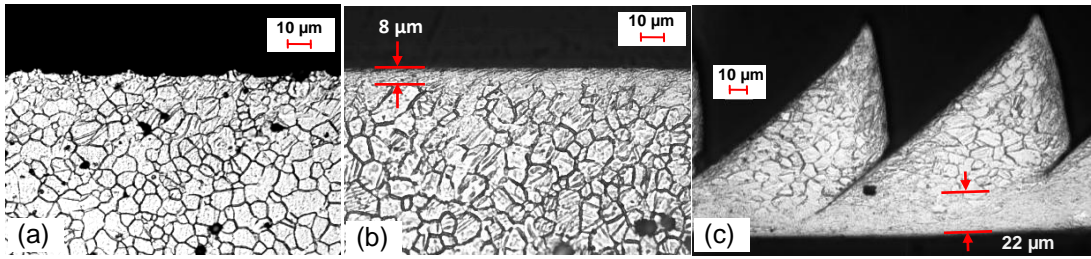


Fig. 2. Microstructures of AZ31B Mg samples (a) initial, (b) machined surface after cryogenic machining using a cutting tool with 30  $\mu\text{m}$  edge radius and (c) chips from the same condition (cutting speed: 100 m/min; feed rate: 0.1 mm/rev).

### 3.2. Crystallographic orientation

Corrosion rates of AZ31 Mg were shown to be dramatically increased with decreased basal texture intensity on the exposed surface [18]. Fig. 3a shows the evolution of texture on the machined surface caused by cryogenic machining with the 70  $\mu\text{m}$  cutting edge radius tool. The relative heights of the peaks corresponding to the basal plane (0 0 2) were increased significantly after machining. The relative intensity of the basal peak, which was calculated by dividing its absolute intensity by the absolute intensity of the most intense peak (10  $\bar{1}$  1), was used to evaluate the texture changes quantitatively. As shown in Fig. 3b, a strong influence of cutting edge radius on crystallographic orientation was observed under both dry and cryogenic machining conditions. Larger edge radius led to an increase of the relative intensity of the basal peak and the increase was stronger under cryogenic conditions. The formation of strong basal texture was reported on Mg alloys after cryogenic burnishing [11]. Machining with a large edge radius tool induces more ploughing effects on the workpiece and is similar to the burnishing process [10], which leads to the higher intensity of the basal peak. The ploughing effects of cryogenic machining with 70 cutting edge radius tool were the strongest since the forces measured were the largest [15]. It is as expected this cutting condition led to the strongest basal peak and may improve the corrosion resistance significantly [18].

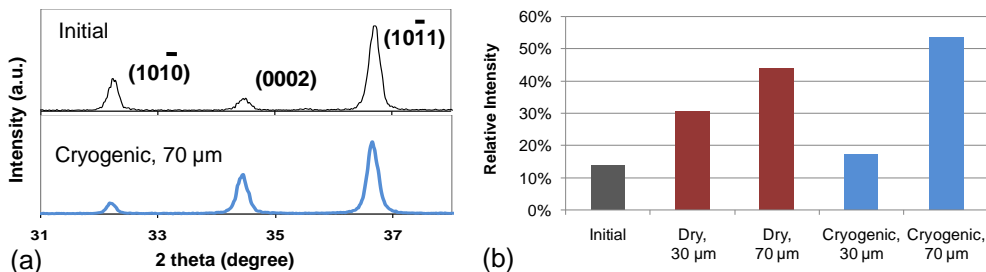


Fig. 3. (a) Evolution of texture on the machined surface caused by cryogenic machining with the 70  $\mu\text{m}$  cutting tool and (b) relative intensity of basal peak before and after machining under different conditions.

### 3.3. Residual stresses

Fig. 4 shows the residual stresses in circumferential and axial directions after machining using cutting tools with two edge radii under both dry and cryogenic conditions. The initial residual stresses (before machining) in both directions were close to zero when the distance from the surface reached about 80  $\mu\text{m}$ . With 30  $\mu\text{m}$  cutting edge radius tool, compressive residual stresses were induced under both dry and cryogenic conditions in the circumferential direction. The maximum value was about -40 MPa and

occurred at about 45  $\mu\text{m}$  below the surface. These two parameters were not changed by cryogenic cooling. Large differences in axial direction were found between dry and cryogenic machining. Dry machining led to formation of tensile residual stresses about 40 MPa in the axial direction while cryogenic machining generated compressive residual stresses about -40 MPa.

Even larger differences between dry and cryogenic machining were found under machining with 70  $\mu\text{m}$  cutting edge radius tool. In the circumferential direction, cryogenic machining induced compressive residual stresses up to more than 200  $\mu\text{m}$  while dry machining was limited to 150  $\mu\text{m}$ . The maximum compressive residual stresses were about -35 MPa, a little smaller than machining with 30  $\mu\text{m}$  edge radius tool. It was reported that larger edge radius led to more compressive residual stresses and thicker compressive layer on *AISI 52100* steel in both directions [19]. However, an opposite trend was observed here for the axial direction under dry machining. Larger edge radius led to a decrease of maximum compressive residual stress from -70 MPa to -60 MPa; the region of compressive residual stresses was also reduced in thickness. Similar to the trend in circumferential direction, cryogenic machining induced deep compressive residual stresses. The influence of edge radius on residual stresses was found to be consistent with literature [19] under cryogenic conditions while inconsistent under dry conditions. The thermal effects induced by larger edge radius outweighed mechanical effects for *AZ31B Mg* alloy during dry machining and thereby led to less compressive residual stresses.

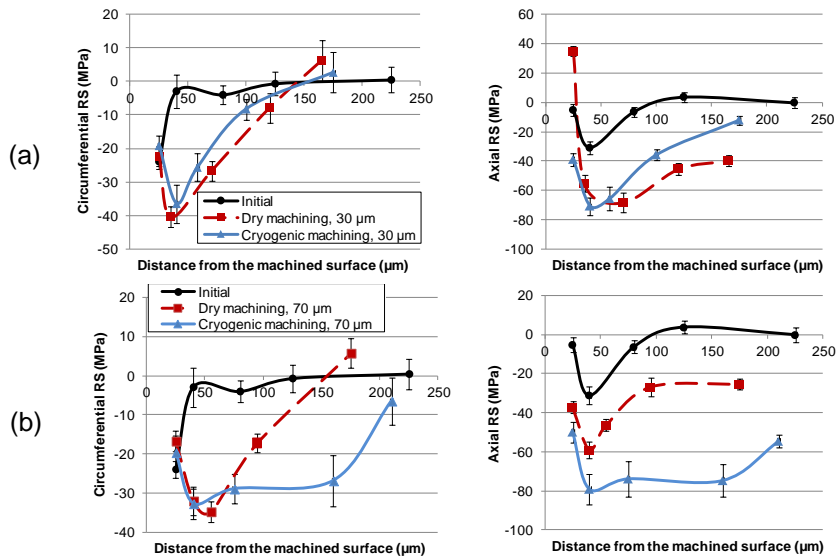


Fig. 4. Measured residual stress in circumferential and axial directions after machining using a cutting tool with (a) 30  $\mu\text{m}$  cutting edge radius; (b) 70  $\mu\text{m}$  cutting edge radius.

#### 4. Conclusions

- Cryogenic machining led to the formation of a grain refinement layer which has an appearance similar to “white layer” formed on steels. The same layer was found in the machined chips near tool-chip interface. Increased cutting edge radius led to a thicker grain refinement layer.
- Larger edge radius led to increased intensity of the basal plane on the machined surface the increase was more remarkable under cryogenic conditions.
- Increased cutting edge radius resulted in deeper layer of compressive residual stresses under cryogenic conditions. Under dry condition, large edge radius led to smaller compressive residual stresses and a decrease in thickness of compressive layer, especially in the axial direction.

Cryogenic machining with large edge radius tool led to enhanced surface integrity on AZ31B Mg alloy in terms of grain size, crystallographic orientation as well as residual stresses. The corrosion performance, which has been proved sensitive to these factors, should be improved significantly. With further development of predictive process models [15, 19], machined products with desired surface integrity can be manufactured to enhance their functional performance without changing their bulk properties and chemical compositions.

## Acknowledgements

The authors would like to thank Air Products and Chemicals for providing the ICEFLY<sup>®</sup> liquid nitrogen delivery system to the Institute of Sustainable Manufacturing at the University of Kentucky. The residual stress measurements were supported by the European Union program FEDER through "Programa Operacional Factores de Competitividade - COMPETE" and the Portuguese Government through "FCT - Fundação para a Ciência e a Tecnologia" under the project with reference PEst-C/FIS/UI0036/2011.

## References

- [1] M'Saoubi R, Outeiro JC, Chandrasekaran H, Dillon OW, Jr., Jawahir IS. A review of surface integrity in machining and its impact on functional performance and life of machined products. *International Journal of Sustainable Manufacturing*. 2008;**1**:203 - 36.
- [2] Jawahir IS, Brinksmeier E, M'Saoubi R, Aspinwall DK, Outeiro JC, Meyer D, Umbrello D, Jayal AD. Surface integrity in material removal processes: Recent advances. *CIRP Annals - Manufacturing Technology*. 2011; **60**: 603-26.
- [3] Wang TS, Yu JK, Dong BF. Surface nanocrystallization induced by shot peening and its effect on corrosion resistance of 1Cr18Ni9Ti stainless steel. *Surf Coat Tech*. 2006;**200**:4777-81.
- [4] Villegas JC, Shaw LL, Dai K, Yuan W, Tian J, Liaw PK, Klarstrom DL. Enhanced fatigue resistance of a nickel-based hastelloy induced by a surface nanocrystallization and hardening process. *Philosophical Magazine Letters*. 2005;**85**:427-38.
- [5] Chandrasekar S, Guo Y, Saldana C, Compton WD. Controlling deformation and microstructure on machined surfaces. *Acta Materialia*. 2011;**59**:4538-47.
- [6] Pu Z, Dillon OW, Jr., Jawahir IS, Puleo DA. Microstructural Changes of AZ31 Magnesium Alloys Induced by Cryogenic Machining and Its Influence on Corrosion Resistance in Simulated Body Fluid for Biomedical Applications. *Proceedings of ASME International Manufacturing Science and Engineering Conference 2010*; **2010**:271-7.
- [7] Witte F. The history of biodegradable magnesium implants: A review. *Acta Biomater*. 2010;**6**:1680-92.
- [8] Wang H, Estrin Y, Fu H, Song G, Zuberova Z. The effect of pre-processing and grain structure on the bio-corrosion and fatigue resistance of magnesium alloy AZ31. *Advanced Engineering Materials*. 2007;**9**:967-72.
- [9] Denkena B, Lucas A. Biocompatible Magnesium Alloys as Absorbable Implant Materials – Adjusted Surface and Subsurface Properties by Machining Processes. *CIRP Annals - Manufacturing Technology*. 2007;**56**:113-6.
- [10] Song GL, Mishra R, Xu ZQ. Crystallographic orientation and electrochemical activity of AZ31 Mg alloy. *Electrochem Commun*. 2010;**12**:1009-12.
- [11] Pu Z, Yang S, Song GL, Dillon Jr OW, Puleo DA, Jawahir IS. Ultrafine-grained surface layer on Mg-Al-Zn alloy produced by cryogenic burnishing for enhanced corrosion resistance. *Scripta Materialia*. 2011;**65**:520-3.
- [12] Outeiro JC, Dias AM, Jawahir IS. On the effects of residual stresses induced by coated and uncoated cutting tools with finite edge radii in turning operations. *Cirp Ann-Manuf Techn*. 2006;**55**:111-6.
- [13] Outeiro JC, Kandibanda R, Pina JC, O.W. Dillon J, Jawahir IS. Size-effects and surface integrity in machining and their influence on product sustainability. *International Journal of Sustainable Manufacturing* 2010;**2**:112 - 26.
- [14] Noyan IC, Cohen JB. Residual stress : measurement by diffraction and interpretation. New York, N.Y.: Springer; 1987.
- [15] Pu Z, Caruso S, Umbrello D, Dillon OW, Jr., Jawahir IS. Analysis of Surface Integrity in Dry and Cryogenic Machining of AZ31B Mg Alloys. *Advanced Materials Research* 2011;**223**:439-48.
- [16] Ramesh A, Melkote SN, Allard LF, Riester L, Watkins TR. Analysis of white layers formed in hard turning of AISI 52100 steel. *Mat Sci Eng a-Struct*. 2005;**390**:88-97.
- [17] Pu Z, Puleo DA, Dillon OW, Jawahir IS. Controlling the Biodegradation Rate of Magnesium-Based Implants through Surface Nanocrystallization Induced by Cryogenic Machining. *Magnesium Technology 2011*: John Wiley & Sons, Inc.; 2011. p. 635-42.
- [18] Xin R, Li B, Li L, Liu Q. Influence of texture on corrosion rate of AZ31 Mg alloy in 3.5 wt.% NaCl. *Mater Design*. 2011;**32**:4548-52.
- [19] Hua J, Umbrello D, Shivpuri R. Investigation of cutting conditions and cutting edge preparations for enhanced compressive subsurface residual stress in the hard turning of bearing steel. *J Mater Process Tech*. 2006;**171**:180-7.